

# Drying of Beulah-Zap lignite

Karl S. Vorres, David L. Wertz\*, Vivak Malhotra†, Yuhong Dang‡,  
J. T. Joseph‡ and Ronald Fisher‡

Chemistry Division, Bldg 211, Argonne National Laboratory, Argonne, IL 60439, USA

\*Department of Chemistry, University of Southern Mississippi, Hattiesburg, MS 39406, USA

†Department of Physics, Southern Illinois University at Carbondale, Carbondale, IL 62901, USA

‡Amoco Oil Co. R&D, Naperville, IL 60566, USA

(Received 25 September 1991; revised 10 February 1992)

Lignite dried in a stream of dry nitrogen at moderate temperatures (20–80°C) loses water in two distinguishable modes. The first mode represents about 80–85% of the loss of moisture. The second represents the other 15–20% lost under these conditions. The rate follows a unimolecular mechanism (like radioactive decay) for each mode. The activation energy for the first mode is close to the heat of vaporization of water. The rate is dependent upon the gas flow around the sample and the weight (or thickness) of the sample. Work at Amoco Oil Company indicated that the oil yield was higher for the dried coal than for raw or partly dried lignite. Work at Southern Illinois University showed that the mechanism was the same when differential scanning calorimetry was used to follow the kinetics of drying. Other work at the University of Southern Mississippi showed that the physical structure of the lignite (measured by X-ray diffraction) is measurably different for the dried and raw materials.

(Keywords: liquefaction; drying; lignite)

Lignite reserves represent an important resource for the production of synthetic liquid fuels. The high reactivity of lignite would indicate a high throughput from a given process train. However, the moisture content of this material has been a concern for efficient processing into liquid hydrocarbons. Furthermore, drying might introduce irreversible changes to the pore structure which could limit the rates of reaction.

This collaborative study has been undertaken to help understand the role of moisture in the liquefaction and also to understand the kinds of changes that take place in the coal particles during drying.

The physical structure of coal consists of an organic matrix and inorganic matter containing an extensive network of pores. The pore network usually contains water. Mraw and Silbernagel<sup>1</sup> suggested that the amount of water present in as-mined coals provides a measure of pore volume. However, Kaji *et al.*<sup>2</sup> examined the water-holding capacity, specific surface area, and pore volume of 13 coals from various locations, ranging from lignite to anthracite, and found no correlation between the water-holding capacity and the pore volume. Assuming that the total coal oxygen is distributed uniformly through the coal and the functional-group oxygen increases with oxygen content, Kaji *et al.* found a linear relationship between the hydrophilic sites and the water-holding capacity of coal. The relationship between the total oxygen content of coal and the water-holding capacity may be fortuitous, since oxygen functional groups are not the only hydrophilic sites in coal<sup>3</sup>. Moreover, the presence of minerals, especially

smectite lattices, and various cations will also strongly influence the coal–water interactions.

Vorres *et al.*<sup>4</sup> and Vorres and Kolman<sup>5</sup> studied the kinetics of vacuum drying of a subbituminous coal and two high-volatile bituminous coals to understand the complex coal water interactions. From isothermal thermogravimetric analysis, i.e. the weight loss vs. time at fixed temperature, Vorres and his co-workers observed that the dehydration of Illinois No. 6 coal in the form of a small lump, <20 mesh (<841  $\mu\text{m}$ ) and <100 mesh (<148  $\mu\text{m}$ ) follows a desorption-kinetics mechanism. Thus they concluded that the rate-controlling mechanism of dehydration is governed by the surface of coal. In addition, they indicated that the particle size and the history of coal also affect the dehydration kinetics of coal.

More recently, Abhari and Isaacs<sup>6</sup> used the thermogravimetric analysis (TGA) technique to explore the drying kinetics of six coals from the Argonne coal-sample series. They used a bulk moisture–pore moisture model to explain the observed drying kinetics for the six coals, in which the order of kinetics, i.e. the order of dehydration, showed a strong dependence on the rank of coal. These researchers assumed that water in coal is held by the physisorption process. This assumption is at variance with temperature-dependent n.m.r. results<sup>7</sup> and the contention of Kaji *et al.*<sup>2</sup>. Even more recently, Vorres *et al.*<sup>8,9</sup> reported the kinetics of drying of lignite in dry nitrogen and evolution of gases from the coal samples. They observed a unimolecular mechanism, with a transition after the loss of about 85% of the water present in the original sample<sup>8</sup>. The transition resulted in a lower rate with the unimolecular mechanism. Studies with the thermobalance and differential scanning calorimeter indicated the same mechanism and transition<sup>8</sup>.

Presented at the 201st ACS National Meeting, Atlanta, Georgia, USA, 14–19 April 1991

Lignite is believed to hold a significant part of the moisture in a gel structure which may collapse on drying.

This paper reports recent results on (1) the kinetics of water desorption from Beulah-Zap lignite coal, as determined by TGA and differential scanning calorimetry (d.s.c.), (2) physical structure changes as observed with X-ray diffraction and (3) the effects on liquefaction due to drying.

The kinetic analysis of d.s.c. was further complemented by determining the mechanism of air drying of lignite coal with the help of an *in-situ* desorption kinetics via Fourier transform infrared (ISDK-FT-i.r.) technique<sup>10</sup>.

## EXPERIMENTAL

### Isothermal thermogravimetry

Coal drying was done with a Cahn model 121 thermobalance attached to an IBM PC/XT micro-computer. Vendor-supplied software was used to monitor the progress of individual runs and to convert data files to a form that could be further studied with Lotus 123.

The data were obtained as files of time, temperature and weight at 10-s intervals. For some of the runs which took more than 10 h, data points were taken at 20-s intervals. Run times varied from 7 to 23 h. Sample sizes varied from about 20 to 160 mg. Temperatures were varied between 20 and 80°C. The gas velocity past the sample was varied from 20 to 160 cm<sup>3</sup> min<sup>-1</sup> in the 25 mm diameter tube. The system was modified so that all of the gas was passed up around the sample before being vented. Initially the experiments (up to run 85) were carried out with a hemispherical or 'round-bottom bucket' quartz pan 12.5 mm in diameter. For the last third of the runs (after run 85), a 'flat-bottom bucket' quartz pan (9.5 mm deep and 9.5 mm diameter) was used to obtain a more uniform thickness of sample. The samples included the two sizes (<100 mesh, or <148  $\mu$ m, and <20 mesh, or <841  $\mu$ m) of the Beulah-Zap Argonne Premium Coal Sample and also one or two small pieces which came from lumps which were stored under nitrogen.

Samples were quickly transferred from opened ampoules which had been kept in a constant-humidity chamber with water at room temperature (293 K) for a minimum of 3 days. In the thermobalance system a period of about 5 min was used to load samples, stabilize the system and initiate data acquisition. The electrical furnace was used for the initial 30 of the 120 experiments. The isothermal operation for long times at near room temperature proved challenging for the furnace temperature control system.

An alternative temperature control system was developed. The furnace was removed and temperature control from the Cahn system was not used. A condenser was made with the same top diameter, length, and gas inlet as well as outlet as the original quartz tube from the Cahn thermobalance. The coolant flowed between a larger-diameter concentric tube which was part of the condenser and the 25 mm inner-diameter tube. An antifreeze solution was circulated from a constant-temperature bath through the condenser to maintain constant temperature during the experiments. This condenser system was much more stable than the furnace and provided very uniform temperature control during the experiments. The condenser was placed in the

position formerly occupied by the furnace, and fitted with the gas inlet at the bottom and gas outlet near the top. The quartz gas flow stabilization tube was kept in place for these experiments. The temperature stability was dependent only on the stability provided by the constant-temperature bath.

The gas atmosphere was cylinder nitrogen (99.99%) or 'house' nitrogen from the evaporation of liquid nitrogen in storage containers, used without further purification and passed over the sample at rates of about 20–160 cm<sup>3</sup> min<sup>-1</sup>.

Data were initially analysed by testing the weight loss as a function of time with 13 different kinetic expressions including geometrical, unimolecular, first- and second-order diffusion to establish a best fit<sup>8</sup>. Regression analysis was used to obtain the kinetic constants. Lotus 123 was used for analysis of individual run data.

### Round-robin sample preparation

In order to compare the results of drying with several experimental and instrumental techniques, a set of samples was prepared and distributed. Batches of 25 g of <100 mesh (<148  $\mu$ m) lignite were dried in vacuum at room temperature. One batch was dried for 4 h, and the other for 24 h. The samples were brought to atmospheric pressure under nitrogen, quickly transferred to a nitrogen-filled glove bag, and transferred to previously dried screw-cap vials. The vials were further sealed with tape around the cap. These samples were distributed to the University of Southern Mississippi for X-ray diffraction studies and Amoco Oil Company for liquefaction studies and comparison with fresh lignite sample.

## RESULTS AND DISCUSSION

### Isothermal thermogravimetry

A typical plot of sample weight and temperature versus time is given in Figure 1. The data were normalized to 1 g of starting sample. The best fit of the data was obtained with a unimolecular decay kinetic expression. This mechanism involves the transformation of a single species, in this case, apparently, water liquid to vapour. Plots of ln(water left) versus time gave a characteristic shape. The plot indicates a consistent slope for the initial ~85% of the moisture loss. A transition then occurs; beyond which the rate is reduced to a fraction of the

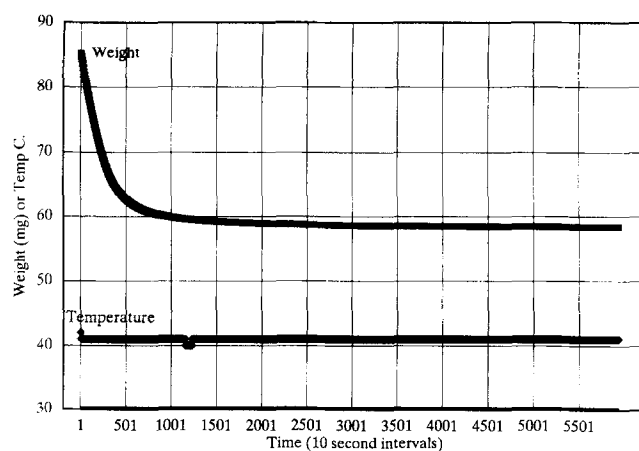


Figure 1 Weight loss for lignite dried in nitrogen at 41°C (run 89, <100 mesh, 80 mg, 20 cm<sup>3</sup> min<sup>-1</sup> with flat-bottom bucket)

earlier rate. Figure 2 shows a typical plot of  $\ln(\text{water left})$  as a function of time.

These data may be analysed in a manner similar to that for a mixture of two radioactive materials of different half-lives. The moisture loss then represents the release of two kinds of water. A sharp transition would indicate that the two kinds were independent of each other. There was a transition period which indicated some exchange between the two types of water. The latter part of the experiment represents the loss of the more strongly held water. The data for that moisture release can be extrapolated to the beginning of the run. The moisture lost from the strongly held water can be subtracted from the total moisture loss to obtain the rate for the loss of the more easily released water. The discussion refers to the first segment as the initial rapid loss, and the second segment as the much slower loss characterized by the second straight segment of the  $\ln(\text{water left})$  versus time plot. All plots give the rate data for the initial rapid loss of moisture.

The initial total rates are similar for different particle sizes if the sample weight and gas velocity are held constant. Table 1 indicates the similarity in rates for 150 mg samples in the hemispherical quartz pan. Activation energies are also given, from regression analysis for each particle size.

The activation energy,  $E_a$ , calculated from these data averages  $8.5 \text{ kcal mol}^{-1}$ , which is close to the heat of vaporization of water. The data are shown in Figure 3, with run numbers indicated by the data points.

The rate is a function of the size of the sample and the gas velocity around the sample. The size of the sample affects the depth of the material through which the moisture must diffuse to escape. The normalized rates are inversely proportional to the sample size. The rate is directly proportional to the gas velocity, since the more rapidly moving stream is more effective in removing the water molecules or limiting the opportunity for rehydration.

Varying the sample weight also varies the depth of the sample in the container. Figures 4–7 indicate the change in total rates of moisture loss as the sample weight is changed at different temperatures and gas flow rates around the sample. The rate in terms of mass of water lost per gram of sample in a given time is greater for the smaller, and therefore thinner, samples. The probability of a water molecule recombining with the lignite rather than leaving the sample diminishes as the diffusion path is shortened.

Data obtained with <20 mesh material at different gas velocities are consistent with the data for <100 mesh material, as shown in Figure 8.

A series of experiments was carried out with distilled water in place of the coal sample to establish an experimental reference value for the heat of vaporization of water. Sample weights were about 100 mg. The results are indicated in Figure 9. Data at 40, 60 and  $80^\circ\text{C}$  gave a value of  $6.9 \text{ kcal mol}^{-1}$  for the activation energy for water vaporization, compared with a literature value of  $9.7 \text{ kcal mol}^{-1}$ . This lower value is slightly less than the range of values obtained in the experiments with the lignite. The values at  $30^\circ\text{C}$  were lower. This difference in values reflects the experimental error and the difference in technique used for determination of the value.

Figures 10–13 show the data plotted for the first segment of total moisture loss for the four different

**Table 1** Rate constants and activation energies for total moisture loss, first segment

Sample size	Rate constant ( $\text{mg}(\text{H}_2\text{O}) \text{ g}(\text{sample})^{-1} (10 \text{ s})^{-1}$ ) at a temperature ( $^\circ\text{C}$ ) of			$E_a$ ( $\text{kcal mol}^{-1}$ )
	20	40	80	
< 100 mesh	0.00009	0.00024	0.00099	8.2
< 20 mesh	0.00007	0.00024	0.00131	10.0
Lump	0.00010	0.00023	0.00085	7.3

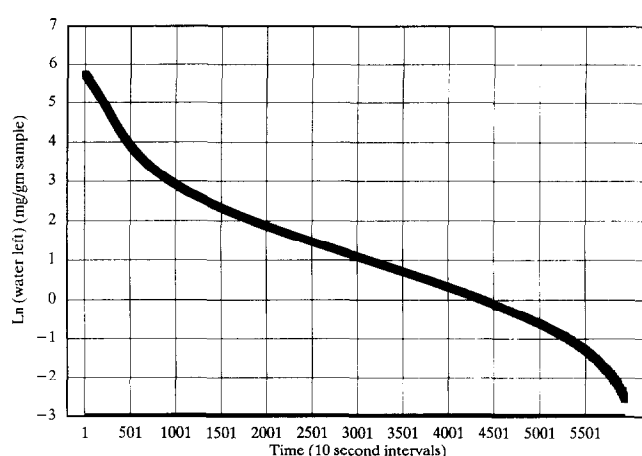


**Figure 2** First-order rate plot for lignite dried in nitrogen at  $41^\circ\text{C}$  (run 89, <100 mesh, 80 mg,  $20 \text{ cm}^3 \text{ min}^{-1}$  with flat-bottom bucket)

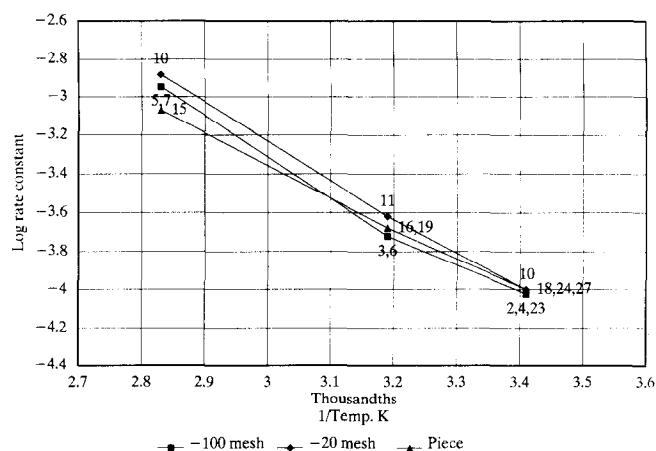


**Figure 3** Arrhenius plot for lignite dried in nitrogen (150 mg samples at 20, 40 and  $80^\circ\text{C}$ , round-bottom bucket; sample sizes and run numbers indicated)

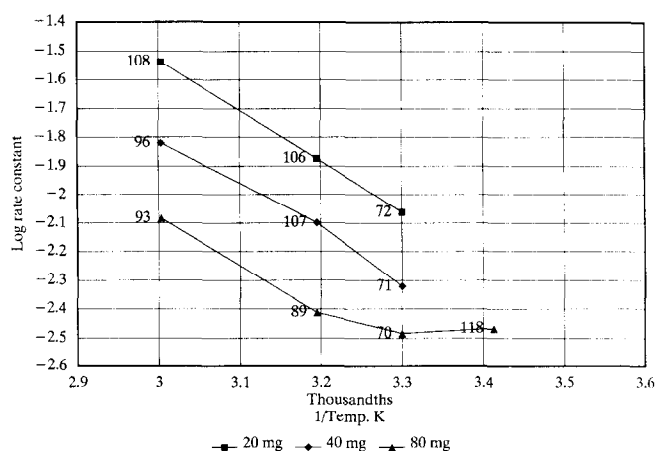


**Figure 4** Arrhenius plot for lignite dried in nitrogen (nitrogen flow rate  $20 \text{ cm}^3 \text{ min}^{-1}$ ; <100 mesh samples at 20, 30, 40 and  $80^\circ\text{C}$ ; sample weights and run numbers indicated)

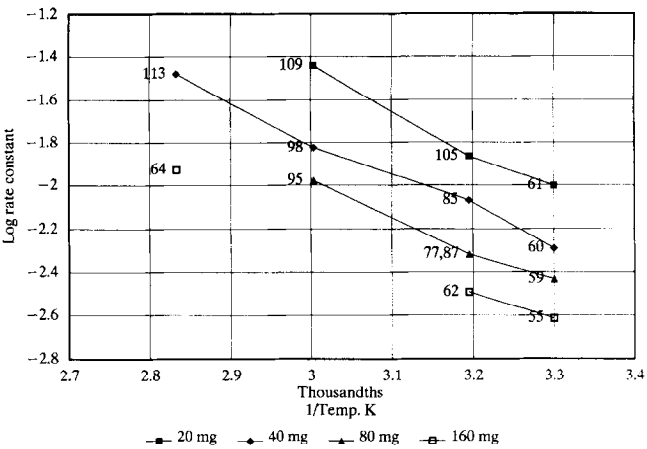


**Figure 5** Arrhenius plot for lignite dried in nitrogen (nitrogen flow rate 40 cm<sup>3</sup> min<sup>-1</sup>; <100 mesh samples at 20, 30, 40 and 80°C; sample weights and run numbers indicated)

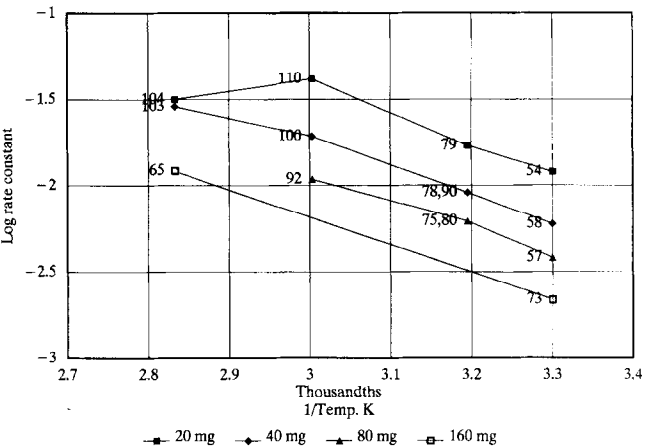


**Figure 6** Arrhenius plot for lignite dried in nitrogen (nitrogen flow rate 80 cm<sup>3</sup> min<sup>-1</sup>; <100 mesh samples at 20, 30, 40 and 80°C; sample weights and run numbers indicated)

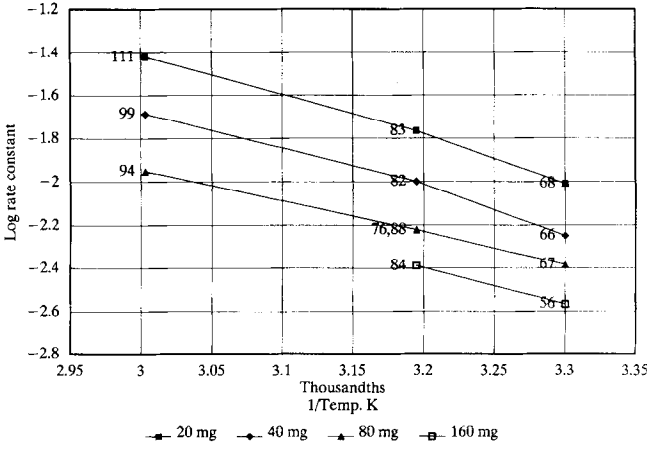


**Figure 7** Arrhenius plot for lignite dried in nitrogen (nitrogen flow rate: 160 cm<sup>3</sup> min<sup>-1</sup>; <100 mesh samples at 20, 30, 40 and 80°C; sample weights and run numbers indicated)

constant gas velocities. The lines are almost parallel and indicate an average activation energy of 8.0 kcal mol<sup>-1</sup>. The higher gas velocities are able to remove water molecules more effectively and increase the rate of drying.

The use of vacuum to remove moisture was seen in one run to be capable of much more rapid removal of water than a stream of dry nitrogen. The ratio of the rate

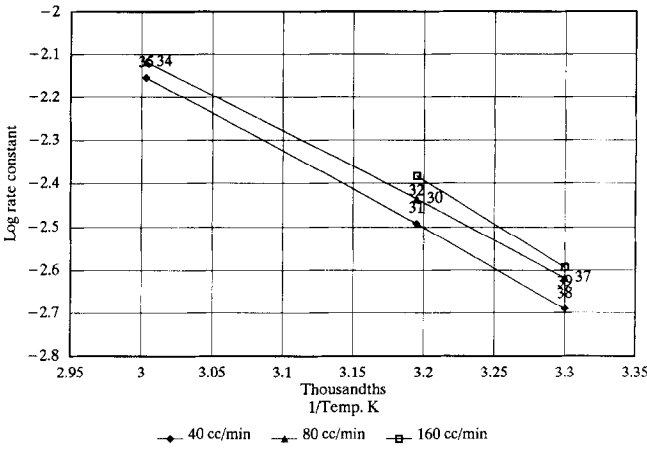


**Figure 8** Arrhenius plot for lignite dried in nitrogen (150 mg samples, <20 mesh, at 20, 40 and 80°C, round-bottom bucket; flow rates and run numbers indicated)

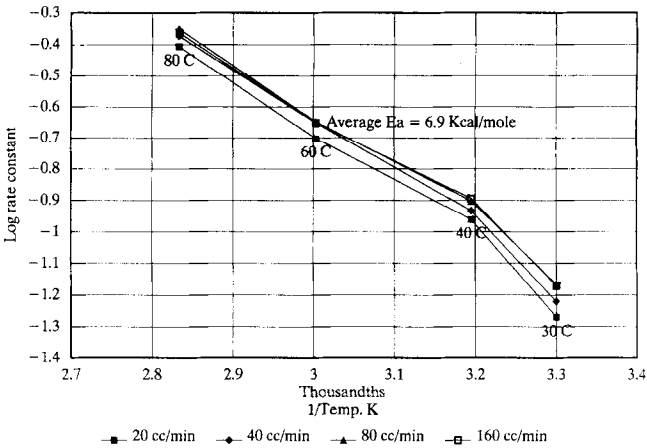


**Figure 9** Arrhenius plot for water evaporated in nitrogen (100 mg samples in flat-bottom bucket; temperatures and flow rates indicated)

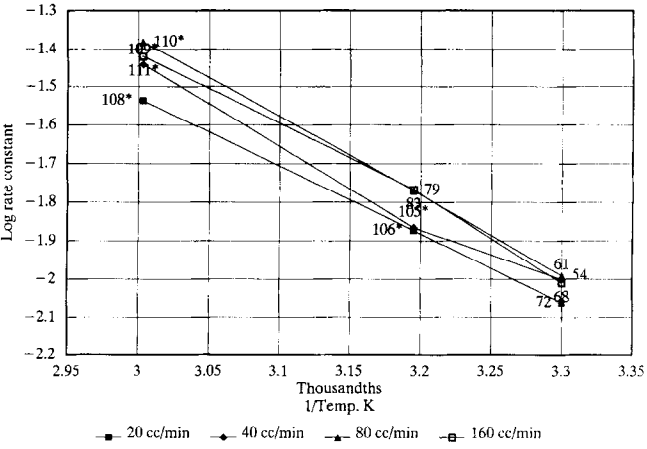


**Figure 10** Arrhenius plot for lignite dried in nitrogen (20 mg samples, <100 mesh, at 30, 40 and 60°C; gas flow rates and run numbers indicated)

coefficients is at least 10, and would imply a rate advantage to this technique for engineering for rapid processing of pulverized fuel.

The initial removal of about 85% of the moisture with a given rate and unimolecular mechanism, followed by a transition to a lower rate with the same mechanism, could be due to the presence of two types of water. A

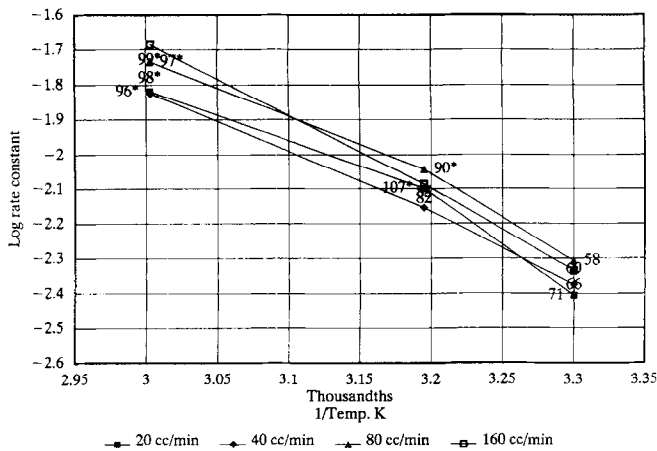


**Figure 11** Arrhenius plot for lignite dried in nitrogen (40 mg samples, <100 mesh, at 30, 40 and 60°C; gas flow rates and run numbers indicated; asterisks indicate runs with the flat-bottom bucket)

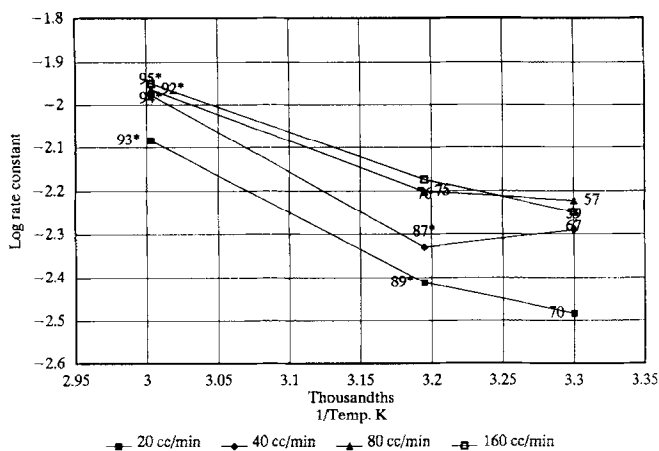


**Figure 12** Arrhenius plot for lignite dried in nitrogen (80 mg samples, <1000 mesh, at 30, 40 and 60°C; gas flow rates and run numbers indicated; asterisks indicate runs with the flat-bottom bucket)

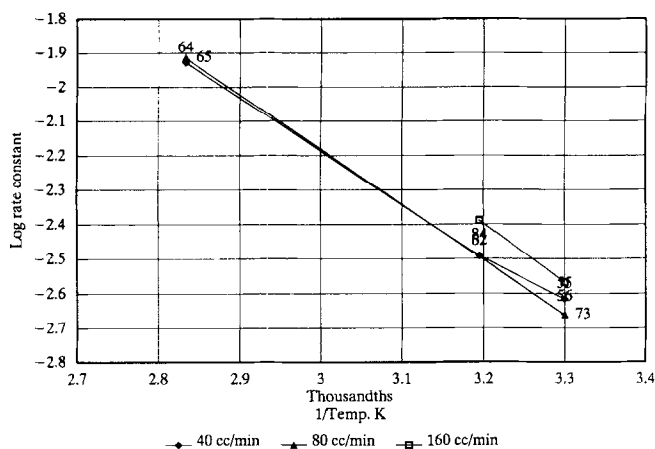


**Figure 13** Arrhenius plot for lignite dried in nitrogen (160 mg samples, <100 mesh, at 30, 40 and 80°C; gas flow rates and run numbers indicated)

more readily released type, such as that found in the central part of larger water-filled pores, would be lost initially. Another type held at functional groups or active sites on the surface would be released more slowly. This type of situation could lead to the observed behaviour. The somewhat gradual transition could imply some exchange between the two types of water.

This behaviour might also be observed if the open pores which provide the escape path of the water molecules became partly blocked due to collapse of the gel structure containing moisture or some of the pores themselves. The gel structure debris may partly block the pores, restricting outward diffusion and reducing the rates.

The activation energy for total loss of moisture and for the more easily lost water is close to the heat of vaporization of water, indicating that the rate of moisture loss is limited by the transfer of energy to the molecules for vaporization.

The unimolecular mechanism implies, by analogy with radioactive decay, that all water molecules have an equal probability of vaporizing at any instant. However, not all molecules are near the surface. The intuitive picture of water molecules vaporizing from a liquid-gas interface leads to the expectation that only liquid molecules at the interface would vaporize. The situation raises the question of some very dynamic equilibrium which permits energy to be transferred to the surface by any molecule.

The attempts to obtain an activation energy for the second segment were not successful. The data points for a given set of mass and gas velocity conditions at different temperatures did not give straight lines on the typical Arrhenius plot of  $\ln k$  vs.  $1/T$ . This behaviour indicates that the rate for the second segment may be dependent on the nature of the drying process during the first segment. Furthermore, the observed rate involves some variation in the drying process or structure of the lignite.

It has been assumed that all of the mass loss in the experiments was due to moisture loss. Future work will examine the possible evolution of other gases including carbon dioxide and methane. The evolution of carbon dioxide from the sample over time has not been sufficient to cause a significant mass loss<sup>9</sup>.

The form of the rate expression is similar to that obtained by Abhari and Isaacs<sup>6</sup>; however, their expression for the rate of water loss involved a varying exponent:

$$-dW/dt = kW^n$$

where  $n$  had values between 1.3 and 2.4 for the six lowest-rank coals. The experimental conditions were different in their study, in that the samples were taken directly from the ampoule and were not equilibrated with water before the runs. The gas flow rate was indicated to be  $500 \text{ cm}^3 \text{ min}^{-1}$ , which is beyond the range used in this study, and may or may not be comparable, depending on the diameter of their TGA reaction vessel.

#### X-ray diffraction studies

The X-ray diffraction studies carried out at the University of Southern Mississippi shown in Figure 14 indicate that the physical structure of the coal (not the inorganic material) changes on drying. Further, the reduced 'noise' level associated with the diffraction pattern indicates that there is a greater regularity in the dried coal than the raw or partly dried material. Further studies of the diffraction data are under way to provide additional insight into the changes that have been observed.

The peak at  $22^\circ$  is due to an internal standard. The peak at  $14^\circ$  is due to the 002 plane of graphitic material associated with coal samples. Note that the peak shape

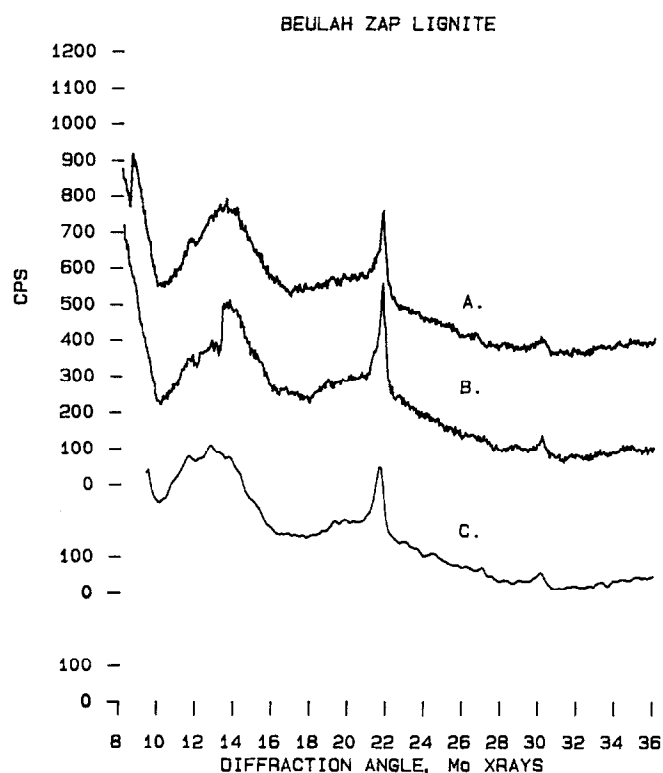


Figure 14 X-ray diffractograms indicating changes in physical structure on drying lignite: A, raw lignite; B, partly dried lignite; C, dried lignite

for untreated lignite is reasonably symmetrical, implying a distribution of spacings about an average value. The partly dried material has a distorted shape for the 002 peak, indicating that the larger planar spacings are no longer present in the sample. In the dried sample the peak is again relatively symmetrical.

#### Liquefaction studies

The oil yield was measured by Amoco Oil Co. at the Naperville Research Center. Small samples were added to tetralin, and the material was heated under hydrogen at 6.9 MPa to 400°C for 4 h. The product gases were recovered and analysed by gas chromatography. The liquid and residual material were extracted with a series of solvents to give oil, preasphaltene and asphaltene fractions.

The studies indicated that the different coal samples did give different oil yields, as well as different preasphaltene and asphaltene yields. The initial data indicate that the raw and partly dried samples gave higher preasphaltene and asphaltene yields than the dried material, with the highest yields for the partly dried sample. Conversely, the oil yield was highest for the dried sample, lowest for the partly dried material and intermediate for the starting material. The data are given in Table 2. The total of oil, preasphaltene and asphaltene fractions was almost the same for all samples. The gas yield was the same for the two moist materials and higher than for the dried material, suggesting a role of moisture in gas production. Hydrogen diminishes for dried coal, while carbon monoxide increases. Methane and higher hydrocarbons remain about the same for all levels of dryness, suggesting that they are released by some mechanism which is not dependent on moisture, i.e. they may simply be dissolved in the matrix. Carbon dioxide

Table 2 Initial liquefaction results

Coal condition	Raw	High moisture	Low moisture
Moisture (wt%)	32.2	23.9	0.3
Products (wt%)			
Oil	24	21	31
Asphaltenes	24	25	20
Preasphaltenes	11	13	7
Unconverted	31	31	33
Total gases	10.5	10.5	8.5
Gases by type			
H <sub>2</sub>	0.209	0.196	0.156
CO	0.238	0.276	0.340
CH <sub>4</sub>	0.486	0.474	0.480
CO <sub>2</sub>	5.373	5.543	4.849
C <sub>2</sub> H <sub>6</sub>	0.163	0.166	0.154
C <sub>3</sub> H <sub>8</sub>	0.056	0.055	0.054
C <sub>3</sub> H <sub>6</sub>	0.011	0.011	0.009

yield increased for the partly dried material and then decreased for the dry material, suggesting two competing reactions.

#### CONCLUSIONS

A number of conclusions follow from this study:

1. The lignite drying kinetics follow a unimolecular rate law which is first order in the water in the sample.
2. There are two segments in the dehydration kinetics plots, and each follows a unimolecular rate law.
3. The first drying segment includes about 80–85% of the water loss.
4. The second drying segment includes most of the remaining water and occurs at a variable fraction of the rate of the first segment.
5. The mechanism is unchanged over the range 20–80°C.
6. The activation energy for the initial moisture loss is about 8–9 kcal mol<sup>-1</sup>.
7. The experimental value for activation energy for water vaporization was 6.9 kcal mol<sup>-1</sup>, for comparison.
8. A water-jacketed heating system provides superior temperature control compared with the conventional furnace in this temperature range.
9. The rate of drying is sensitive to the gas velocity over the sample.
10. The rate of drying is dependent on the sample size and the sample depth.
11. Rates are generally independent of particle size for lumps and <20 and <100 mesh samples.
12. The same mechanism is observed for differential scanning calorimetry measurements.
13. X-ray powder diffraction measurements show structural changes during the drying process.
14. Drying improves the oil yield from lignite samples, as a result of hydrogenation.

#### ACKNOWLEDGEMENTS

K.S.V. gratefully acknowledges the support of the US Department of Energy, Pittsburgh Energy Technology Center, for the part of the work dealing with the kinetics of drying. Thanks are also due to Don Molenda, Randy Pippen, Larry Jefferson and John Schwartz (high-school teachers) for participation in the summer programme

at ANL. Robert McBeth prepared the vacuum-dried samples.

## REFERENCES

- 1 Mraw, S. C. and Silbernagel, B. G. *Proc. Am. Inst. Phys.* 1981, **70**, 332
- 2 Kaji, R., Maranaka, Y., Otsuka, K. and Hishinuma, Y. *Fuel* 1986, **65**, 288
- 3 Laskowski, J. S. *Am. Chem. Soc. Div. Fuel Chem. Prepr.* 1987, **32**, 367
- 4 Vorres, K. S., Kolman, R. and Griswold, T. *Am. Chem. Soc. Div. Fuel Chem. Prepr.* 1988, **33**, 333
- 5 Vorres, K. S. and Kolman, R. *Am. Chem. Soc. Div. Fuel Chem. Prepr.* 1988, **33**, 7
- 6 Abhari, R. and Isaacs, L. L. *Energy Fuels* 1990, **4**, 448
- 7 Unsworth, J. F., Fowler, C. S., Heard, N. A., Weldon, V. L. and McBrierty, V. J. *Fuel* 1988, **67**, 1111
- 8 Vorres, K. S., Molenda, D., Dang, Y. and Malhotra, V. M. *Am. Chem. Soc. Div. Fuel Chem. Prepr.* 1991, **36**, 108
- 9 Vorres, K. S. 'Proc. 1989 Int. Conf. Coal Science', Vol. II, p. 1083
- 10 Mu, R. and Malhotra, V. M. *Fuel* 1991, **70**, 1233